Polymer Solvent Dynamic Effects on an Electron-Transfer Cross-Reaction Rate at a Redox Polymer/Polymer Solution Interface

Honghua Zhang† and Royce W. Murray*

Contribution from Kenan Laboratories of Chemistry, University of North Carolina, Chapel Hill, North Carolina 27599-3290. *Received July 13, 1992*

Abstract: Electron-transfer cross-reaction rate constants (k_{12}) for the oxidation of polyether solutions of [Fe(4,7-dimethylphenanthroline)$_3$]$^{2+}$ at a poly[Os(bpy)$_2$(vpy)$_2$]$^{3+}$ redox polymer surface have been measured as a function of the polyether solvent employed. Previous measurements in monomer solvents produced values of k_{12} adherent to a theoretical model incorporating the monomer solvent longitudinal relaxation time (τ_L), dielectric constant, and the cross-reaction free energy. Values of k_{12} are smaller in polyether solvents, consistent with reaction rate control by solvent dipole relaxation times (τ_L') that are longer in polymeric relative to monomeric solvents. Further, k_{12} decreases under conditions where polyether chain segment fluctuations are expected to be slowed, e.g., longer polyether chain length and increased $LiClO_4$ and $Zn(CF_3SO_3)_2$ electrolyte concentrations. The diffusion coefficient of the iron complex in the polymer solution, for analogous reasons of slowed chain segmental mobility, also decreases in longer polyether chain solvents and at higher electrolyte concentrations.

We recently reported[1] rate constant data for the electron-transfer cross-reaction:

$$\text{Pt/poly[Os]}^{3+} + [\text{Fe(Me}_2\text{phen)}_3]^{2+} \xrightarrow{k_{12}} \text{Pt/poly[Os]}^{2+} + [\text{Fe(Me}_2\text{phen)}_3]^{3+} \quad (1)$$

where poly[Os] refers to a film of poly[Os(bpy)$_2$(vpy)$_2$]$^{2+}$ (bpy = 2,2′-bipyridine; vpy = 4-vinylpyridine) formed by electropolymerization[2] onto a Pt microdisk electrode and maintained in the poly[Os(bpy)$_2$(vpy)$_2$]$^{3+}$ state by control of the electrode potential. The rate was studied as a function of the solvent in which the [Fe(Me$_2$phen)$_3$]$^{2+}$ complex (Me$_2$phen = 4,7-dimethylphenanthroline) was dissolved. In monomeric solvents (e.g., acetonitrile, acetone, methylene chloride, dimethyl sulfoxide, pyridine, dimethoxyethane, or propylene carbonate), the cross-reaction rate constant k_{12} varied[1] with monomer solvent longitudinal relaxation times (τ_L) in a manner consistent with theory for rate control[3] by slow solvent repolarization.

Having established that reaction 1 responds to solvent dipole relaxation rates, we also measured[1] k_{12} when the iron complex was dissolved in the short-chain polyether solvent $CH_3O(CH_2CH_2O)_8CH_3$ (Me$_2$PEG-400). We interpreted the smaller k_{12} value observed in the polyether solvent as reflecting control by a slower rate of solvent dipole reorganization. The reorganization is slower because the ether dipole is embedded in a polymer chain, and its motions, relative to those of the electron-transfer cross-reactants, require concurrent, articulated segmental (or subsegmental) motions of the polymer chains solvating the reactants. Taking the monomer solvent τ_L-controlled behavior of k_{12} as a calibration, we estimated[1] an average relaxation time τ_L' of 22 ps for the ether dipoles in 0.1 M $LiClO_4$/Me$_2$PEG-400 solution.

Our study[1] of reaction 1 follows a rapidly evolving body of research on solvent dynamics effects on the rates of electron-transfer reactions and on fast chemical processes.[3] Theory predicts that, in the adiabatic regime, the rates of outer-sphere electron transfers in which the nuclear motions involved are those of the solvent sheath are inversely proportional to the solvent longitudinal relaxation time, τ_L. Substantial attention has been given in theoretical[4] and experimental work[5-8] to monomeric solvents; there is, on the other hand, little information available on electron-transfer dynamics in more complex polar solvent environments like polymer electrolytes.[9] Intuitively, a wide range of dipole fluctuation timescales become accessible with polymeric solvents, and, significantly, these timescales should be systematically manipulable based on known features of polymer electrolyte dynamics including how polyether chain segmental mobility is reflected in ionic conductivities[9] and solute diffusion coefficients[10] in these media. There are, however, two identifiable constraints to this idea. In extremes of slow polymer solvent dipole relaxations and of fast electron transfers, the electron transfer may become nonadiabatic because[11] the attendant very slow diffusion and reactant collision rates act to promote long distances of electron transfer. Secondly, in relation to monomer solvents, the dipolar motions in polymer solvents are more complex and potentially multimode.

A polymer dynamics parameter used to characterize polymer chain segmental mobility is the renewal time[12] τ_r. The renewal time (or its average over a distribution of relaxation times) should increase with chain length for short-chain oligomers.[13] Relaxation times for chain segmental motion have been studied in pure polyethers and in their electrolyte solutions ("polymer electrolytes") and ordinarily are increased in the latter. Brillouin scattering measurements[14-16] in (MW 4000) poly(propylene oxide) gave

† Present address: Enzyme Technology Research Group, Inc., 710 Main St., Durham, NC 27701.

(1) Zhang, H.; Murray, R. W. *J. Am. Chem. Soc.* **1991**, *113*, 5183.
(2) Murray, R. W. *Annu. Rev. Mater. Sci.* **1984**, *14*, 145.2.
(3) (a) Maroncelli, M.; MacInnis, J.; Fleming, G. R. *Science* **1989**, *243*, 1674. (b) Bagchi, G. *Annu. Rev. Phys. Chem.* **1989**, *40*, 115. (c) Weaver, M. J.; McManis, G. E. *Acc. Chem. Res.* **1990**, *23*, 295. Weaver, J. J. *Chem. Rev.* **1990**, *92*, 463.
(4) (a) Calef, D. F.; Wolynes, P. G. *J. Phys. Chem.* **1983**, *87*, 3387. (b) Zusman, L. D. *Chem. Phys.* **1980**, *49*, 295. (c) Alexandrov, I. V. *Chem. Phys.* **1980**, *51*, 449. (d) Van der Zwan, G.; Hynes, J. T. *J. Chem. Phys.* **1982**, *76*, 2993. (e) Hynes, J. T. *J. Phys. Chem.* **1986**, *90*, 3701.
(5) (a) Gennett, T.; Milner, D. F.; Weaver, M. J. *J. Phys. Chem.* **1985**, *89*, 2787. (b) Hupp, J. T.; Weaver, M. J. *J. Phys. Chem.* **1985**, *89*, 2795. (c) McManis, G. E.; Golovin, M. N.; Weaver, M. J. *J. Phys. Chem.* **1986**, *90*, 6563. (d) Neilson, R. M.; McManis, G. E.; Golovin, M. N.; Weaver, M. J. *J. Phys. Chem.* **1988**, *92*, 3441. (e) McManis, G. E.; Weaver, M. J. *Chem. Phys. Lett.* **1988**, *145*, 55. (f) Weaver, M. J.; Phelps, D. K.; Nielson, R. M.; Golovin, M. N.; McManis, G. E. *J. Phys. Chem.* **1990**, *94*, 2949.
(6) (a) Opallo, M. *J. Chem. Soc., Faraday Trans. 1* **1986**, *82*, 339. (b) Kapturkiewicz, A.; Behr, B. *J. Electroanal. Chem.* **1984**, *179*, 187. (c) Kapturkiewicz, A.; Opallo, M. *J. Electroanal. Chem.* **1985**, *185*, 15.
(7) (a) Harrer, W.; Grampp, G.; Jaenicke, W. *J. Electroanal. Chem.* **1986**, *209*, 223. (b) Grampp, G.; Harrer, W.; Jaenicke, W. *J. Chem. Soc., Faraday Trans. 1*, **1987**, *83*, 161. (c) Harver, W.; Grampp, G.; Jaenicke, W. *Chem. Phys. Lett.* **1984**, *112*, 263.
(8) Zhang, X.; Yang, H.; Bard, A. J. *J. Am. Chem. Soc.* **1987**, *109*, 1916.
(9) (a) Armand, M. B. *Annu. Rev. Mater. Sci.* **1986**, *16*, 245. (b) Vincent, C. A. *Prog. Solid State Chem.* **1987**, *17*, 145. (c) Ratner, M. A.; Shriver, D. F. *Chem. Rev.* **1988**, *88*, 109.
(10) Watanabe, M.; Longmire, M. L.; Murray, R. W. *J. Phys. Chem.* **1990**, *94*, 2614.
(11) Watanabe, M.; Wooster, T. T.; Murray, R. W. *J. Phys. Chem.* **1992**, *96*, 5886.
(12) Ratner, M. A. *Polymer Electrolyte Reviews-1*; MacCallum, J. R., Vincent, C. A., Eds.; Elsevier Applied Science: New York, 1989.
(13) Fox, T. G.; Flory, P. J. *J. Appl. Phys.* **1950**, *21*, 581; *J. Am. Chem. Soc.* **1948**, *70*, 2384.
(14) (a) Sandahl, J.; Schantz, S.; Borjesson, L.; Torell, L. M.; Stevens, J. R. *J. Chem. Phys.* **1989**, *91*, 655. (b) Borjesson, L.; Stevens, J. R.; Torell, L. M. *Polymer 28*, **1987**, 1803.
(15) Yano, S.; Rahalkar, R. R.; Hunter, S. P.; Wang, C. H.; Boyd, R. H. *J. Polym. Sci.* **1976**, *14*, 1877.

0002-7863/93/1515-2335$04.00/0

"local structure relaxation times" between 50 ps and 1 ns. Proton NMR correlation times for polymer chain motion in PEO-based electrolyte are ca. 400 ps.[17] Microwave studies of $P(EO)_8/NH_4CF_3SO_3$ gave a characteristic renewal time of ca. 100 ps.[18] These relaxation times are significantly longer than those of the typical monomer solvent τ_L (0.2 to 6 ps); the smaller of them is close to our k_{12}-based estimate[1] of the 22 ps relaxation time in the short-chain polyether Me_2PEG-400.

This paper presents further measurements of k_{12} of reaction 1, aiming at establishing a more detailed connection between polymer-phase electron-transfer rate constants and the dynamics of polymer chain segment or subsegment motions. We do this, firstly, by varying chain length in the $CH_3O(CH_2CH_2O)_nCH_3$ family, from $n = 1$ (dimethoxyethane, a monomer) to $n = 22$ (Me_2PEG-2000, a hard waxy solid at room temperature), and, secondly, by varying the concentration of supporting electrolyte in Me_2PEG-400. It is known[9,14-16] that dissolved, ether-coordinated alkali metal cations tend to depress polyether chain flexibility. Thirdly, since physical diffusivities[10] of polyether phase solutes also indirectly reflect values of polymer chain mobility, we measure diffusivity (D_s) of the $[Fe(Me_2phen)_3]^{2+}$ complex in the polyether solutions. The diffusivities parallel the k_{12} results. Fourthly, the temperature dependencies of k_{12} and of D_s in Me_2PEG-400/$LiClO_4$ are compared.

Experimental Section

Chemicals. Ethylene glycol dimethyl ether, 2-methoxyethyl ether, triethylene glycol dimethyl ether, and tetraethylene glycol dimethyl ether (Aldrich) and $Zn(CF_3SO_3)_2$ (zinc trifluoromethanesulfonate) were used as received. Poly(ethylene glycol) dimethyl ethers (Me_2PEG-400, nominal average MW 400; Me_2PEG-1000, nominal average MW 1000; Me_2PEG-2000, nominal average MW 2000; Polysciences) were dried in vacuo (50 °C). Et_4NClO_4 and $LiClO_4$ were recrystallized and dried in vacuo (50 °C). The metal complexes $[Os(bpy)_2(vpy)_2](PF_6)_2$ and $[Fe(Me_2phen)_3](PF_6)_2$ were prepared as previously described.[19]

Measurements. Polymer-phase voltammetry[20] was conducted using the tips of 10-μm (diameter) Pt wire (working electrode, sealed in soft glass tubing) and 26-gauge Pt and Ag wire auxiliary and pseudo-reference electrodes, respectively, all sealed together in an epoxy cylinder. In some experiments, the Ag wire reference was isolated behind a porous Vycor junction to avoid reference electrode drift.

Electrochemical equipment consisted of a locally constructed small current potentiostat,[21] a Faraday cage, and PAR 175 universal programmer. Viscosities were measured using Cannon Ubbelohde-type viscometers and refractive indexes with an Abbe refractometer (AO Scientific Inst.). Cell temperatures were controlled at 23 ± 0.2 °C and at elevated temperatures with a Neslab circulator.

Electropolymerization. $Poly[Os(vpy)_2(bpy)_2](ClO_4)_2$ films were formed on the 10-μm Pt microdisk by electropolymerization from Et_4NClO_4/acetonitrile solutions of $[Os(bpy)_2(vpy)_2]^{2+}$ as shown before.[19,22] Conditions of 50-V/s potential sweep rates and dilute $[Os(bpy)_2(vpy)_2]^{2+}$ monomer solutions (0.2 to 0.5 mM) aid in confining redox polymer deposition to the Pt microdisk electrode. Deposition of polymer on the surrounding glass shroud is undesirable since it leads to a supplemental lateral (cylindrical geometry) current flow to the microdisk[22,23] and consequent overestimation of the cross-electron-transfer rate constant k_{12}. The films typically contain 2 to 3×10^{-9} mol/cm² (e.g., 1.6 to 2.4×10^{-17} mol) of $poly[Os(bpy)_2(vpy)_2]^{2+}$ sites as judged from slow potential scan cyclic voltammetry in 0.1 M Et_4NClO_4/CH_3CN. In acetonitrile solvent, the films are stable to Os(II⇌III) cycling, but they are less stable in the polyether solvents as evidenced by a gradual loss of Os(II/III) peak current and increase in reaction 1 currents. Fresh films were accordingly used in all kinetic measurements. An initial period of soaking was also required to moderate film resistance effects in the polyether solvents.

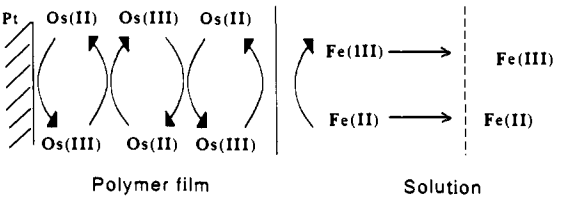

Figure 1. Electron-transfer cross-reaction scheme.

Scheme of Electron-Transfer Cross-Reaction Measurement

In the charge flow scheme (Figure 1) for measurement of k_{12} in reaction 1, the electron-transfer cross-reaction is in series with delivery of Os(III) sites through the redox polymer film (by electron self-exchange between Os(II) and Os(III) sites) and with diffusive delivery of the Fe(II) complex from the bulk solution. The scheme forces current control onto the rate of electron transfer between the diffusing $[Fe(Me_2phen)_3]^{2+}$ solute and the outermost monolayer of $[Os(bpy)_2(vpy)_2]^{3+}$ in the redox polymer film by the following: First, though very thin, the polymer film is relatively defect-free, and, as has been established,[19] the permeation of bulky co-ions such as the iron complex into the redox polymer film is negligible. Secondly, because the interfacial Os(III)/Fe(II) reaction occurs in its thermodynamically unfavorable direction, its rate is slower than the sequential Os(II)/Os(III) charge-delivering self-exchanges within the polymer film. In acetonitrile solvent,[1] for example, the $poly[Os(bpy)_2(vpy)_2]^{3+/2+}$ $E^{\circ\prime}$ is 0.72 V, and the $[Fe(Me_2phen)_3]^{3+/2+}$ $E^{\circ\prime}$ is 0.89 V versus SSCE, so the reaction is disfavored by $\Delta E^\circ = 0.17$ V. ΔE° is somewhat solvent-dependent and in the ether solvents lies above 0.20 V. Thirdly, the normally fast, thermodynamically favored back-reaction of reaction 1 is quenched by rapid removal of product Os(II) sites from the redox polymer/solution interface. This is jointly accomplished by the facile Os(II/III) self-exchange and by the steep concentration gradient and consequent large electron flux created by the very thin redox polymer film. A quantitative justification of the above points was presented earlier.[1,24]

Under these conditions, the limiting current flowing at a $poly[Os(bpy)_2(vpy)_2]^{2+}$-coated Pt microdisk ($I_{LIM}$) is related to the characteristic currents I_{KIN} and I_{MT} for reaction 1 and for $[Fe(Me_2phen)_3]^{2+}$ diffusion, respectively, by[1,22]

$$\frac{1}{I_{LIM}} = \frac{1}{I_{MT}} + \frac{1}{I_{KIN}} = \frac{1}{4rnFD_sC_s} + \frac{1}{nF\pi r^2 k_{12}\Gamma C_s} \quad (2)$$

where C_s and D_s are respectively polyether solution concentration and diffusion coefficient of $[Fe(Me_2phen)_3]^{2+}$, r is microelectrode radius (5 μm), k_{12} is the second-order reaction 1 rate constant (cm³/mol·s), and Γ is the quantity of osmium complex in the outermost monolayer of the $poly[Os(bpy)_2(vpy)_2]^{3+}$ film (taken as 1×10^{-10} mol/cm²). The product $k_{12}\Gamma$ (cm/s), the heterogeneous electron-transfer rate constant for $[Fe(Me_2phen)_3]^{2+}$ oxidation at the redox polymer surface, is converted into second-order units by dividing by 1×10^{-10} mol/cm². The diffusion limited current I_{MT} for $[Fe(Me_2phen)_3]^{2+}$ is measured at a naked Pt microdisk in the same solution as used for the I_{LIM} measurement.

Solvent Dynamics Theory

The previous analysis[1] of solvent dynamics effects in (1) relied on equations[3,4] for an isoenergetic, adiabatic electron transfer:

$$k = K_{pre}\kappa_{el}\nu_n \exp[-\Delta G^{\ddagger}_{Os}/RT] \quad (3)$$

$$\Delta G^{\ddagger}_{Os} = (Ne^2/16\pi\epsilon_0)(1/a - 1/R_h)(1/\epsilon_{opt} - 1/\epsilon_s) \quad (4)$$

$$\nu_n = \tau_L^{-1}(\Delta G^{\ddagger}_{Os}/4\pi RT)^{1/2} \quad (5)$$

(16) Torell, L. M.; Schantz, S. *Polymer Electrolyte Reviews-2*; MacCallum, J. R., Vincent, C. A., Eds.; Elsevier Applied Science: New York, 1989.
(17) (a) Greenbaum, S. G. *Solid State Ionics* **1985**, *15*, 259. (b) Ratner, M. A. *Polym. Electrolyte Rev.* **1987**, *1*, 173.
(18) Ansari, S. M.; Brodwin, M.; Stainer, M.; Druger, S. D.; Ratner, M. A.; Shriver, D. F. *Solid State Ionics*, **1985**, *17*, 101.
(19) Leidner, C. R.; Murray, R. W. *J. Am. Chem. Soc.* **1984**, *106*, 1606.
(20) Geng, L.; Reed, R. A.; Kim, M. H.; Wooster, T. T.; Oliver, B. N.; Egekeze, J.; Kennedy, R.; Jorgenson, J. W.; Parcher, J. F.; Murray, R. W. *J. Am. Chem. Soc.* **1989**, *111*, 1614.
(21) Dayton, M. A.; Wightman, R. M. *Anal. Chem.* **1981**, *53*, 1842.
(22) Feldman, B. J.; Ewing, A. G.; Murray, R. W. *J. Electroanal. Chem.* **1985**, *194*, 63.
(23) Zhang, H. Ph.D. Thesis, University of North Carolina, Chapel Hill, NC, 1991.

(24) Specifically,[1] the available flux of electrons removed from the interface by Os(III/II) polymer film electron self-exchange is $> \sim 10^2$-fold larger than the actual currents due to reaction 1, and the measured rate constants ($k_{12}\Gamma$) do not depend on the polymer film thickness from 1 to 8×10^{-9} mol/cm².

Table I. Solvent Properties and Electron-Transfer Rate Constants for Reaction 1

solvent $CH_3(OCH_2CH_2)_nOCH_3$	ϵ_s[a]	ϵ_{op},[b] 23 °C	η,[b] cP, 23 °C	τ_L,[c] ps	D_s,[d] cm^2/s, 23 °C	$\Delta E°$,[e] 23 °C	$k_{12}\Gamma$,[f] 23 °C	$k^{corr}\Gamma$,[g] cm/s, 23 °C	D_s,[d] cm^2/s, 55 °C	$\Delta E°$,[e] 55 °C	$k_{12}\Gamma$,[f] 55 °C	$k^{corr}_{s}\Gamma$, cm/s, 55 °C
DME (n = 1)	7.20	1.903	0.469	1.7	5.9×10^{-6}	0.227	2.1×10^{-3}	5.3×10^{-3}	1.4×10^{-5}	0.255	1.1×10^{-2}	5.4×10^{-2}
diglyme (n = 2)	(5.79)	1.982	1.122	6.1	2.5×10^{-6}	0.220	6.7×10^{-4}	2.2×10^{-3}				
triglyme (n = 3)		2.024	2.193	6.8	1.4×10^{-6}	0.220	6.0×10^{-4}	1.6×10^{-3}				
tetraglyme (n = 4)	(9.16)	2.051	3.785	7.8	8.2×10^{-7}	0.212	5.6×10^{-4}	1.2×10^{-3}	1.1×10^{-6}	0.245	1.9×10^{-3}	7.2×10^{-3}
Me_2PEG-400 (n = 8)		2.128	14.4	22	1.9×10^{-7}	0.219	1.9×10^{-4}	4.8×10^{-4}	4.2×10^{-7}	0.230	6.6×10^{-4}	1.9×10^{-3}
Me_2PEG-1000 (n = 22)									2.6×10^{-7}	0.237	5.1×10^{-4}	1.4×10^{-3}
Me_2PEG-2000 (n = 44)									2.35×10^{-7}	0.215	4.2×10^{-4}	9.3×10^{-4}

[a] Static dielectric constant for DME is from: *Organic Solvents*, 4th ed.; Wiley-Interscience: New York, 1986. The others (in parentheses) are from: *Industrial Solvent Handbook*; Noyes Data Corp.: Park Ridge, NJ, 1985. [b] Measured in this work, no electrolyte present. [c] Calculated by employing Figure 3B of ref 1 as a working plot representing the relation between k_{12} and τ_L of this cross-reaction. [d] Diffusion coefficient of $[Fe(Me_2phen)_3]^{2+}$. [e] Formal potential difference, $\Delta E° = E°_{Fe(III/II)} - E°_{Os(III/II)}$. [f] Heterogeneous rate constant, uncorrected for variation in $\Delta E°$. [g] Heterogeneous electron-transfer rate constant of reaction 1, normalized to $\Delta E°$ = 0.170 V.

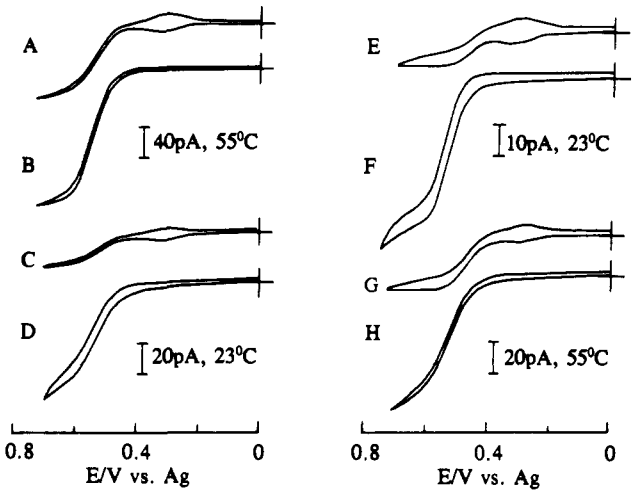

Figure 2. Microelectrode voltammetry (v = 5 mV/s, r = 5 μm) at 23 °C and at 55 °C of (A) microdisk coated with poly$[Os(bpy)_2(vpy)_2]^{2+}$ in 0.08 mM $[Fe(Me_2phen)_3]^{2+}$, 0.1 M $LiClO_4$/DME, 55 °C; (B) naked microdisk in same solution as (A); (C) microdisk coated with poly$[Os(bpy)_2(vpy)_2]^{2+}$ in 0.06 mM $[Fe(Me_2phen)_3]^{2+}$, 0.1 M $LiClO_4$/DME, 23 °C; (D) naked microdisk in same solution as (C); (E) microdisk coated with poly$[Os(bpy)_2(vpy)_2]^{2+}$ in 1.2 mM $[Fe(Me_2phen)_3]^{2+}$, 0.1 M $LiClO_4$/Me_2PEG-400, 23 °C; (F) naked microdisk in same solution as (E); (G) microdisk coated with poly$[Os(bpy)_2(vpy)_2]^{2+}$ in 1.2 mM $[Fe(Me_2phen)_3]^{2+}$, 0.1 M $LiClO_4$/Me_2PEG-400, 55 °C; (H) naked microdisk in same solution as (G).

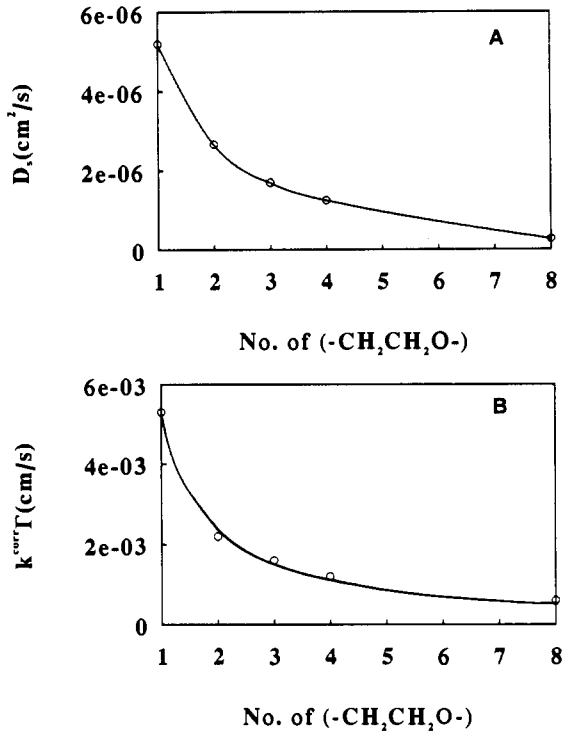

Figure 3. Dependence of (panel A) $[Fe(Me_2phen)_3]^{2+}$ diffusion coefficient, D_s, and (panel B) $k^{corr}\Gamma$ of reaction 1 on the number of ethylene oxide units in the ether solvents.

where the solvent dipole fluctuation rate is introduced[25] by τ_L into the nuclear frequency factor ν_n; K_p is the precursor complex equilibrium constant, κ_{el} the electronic transmission coefficient, ΔG^* the activation free energy which primarily reflects outer-shell solvent reorganization, a the equivalent reactant radius, and R_h the reactant separation (we assume $R_h = 2a$); ϵ_{opt} and ϵ_s are the optical and static dielectric constants for the polyether solvent. Use of these relations for a cross-reaction (i.e., reaction 1) requires correction either to zero reaction energy or to some common value, which can be done since previous studies[9] have shown that k_{12} for reactions like (1) responds to variations in free energy according to the relation[26]

$$k_{12} = (k_{11}k_{22}K_{12}f)^{1/2} \qquad (6)$$

where K_{12} the reaction equilibrium constant equals $\exp[-nF\Delta E°/RT]$ and $f \approx 1$. Small solvent-to-solvent variations $\Delta E°$ $= E°'_{Fe(II/III)} - E°_{Os(II/III)}$ are accounted for by normalizing[1] all reaction energies (i.e., $\Delta E°$) to that in acetonitrile (0.170 V), i.e., $k^{corr}\Gamma = k_{12}$ measured in each polyether times $\exp[-nF(0.170 - \Delta E°)/RT]$.

Results

Microelectrode Voltammetry of the Cross-Reaction in Different Polyethers. Figure 2 shows $[Fe(Me_2phen)_3]^{2+}$ oxidation voltammetry at naked Pt microdisks (curves B, D, F, H) and at Pt microdisks coated with poly$[Os(bpy)_2(vpy)_2]^{2+}$ films (curves A, C, E, G), in a monomer ether solvent DME (curves A–D) and in the polyether solvent Me_2PEG-400 (curves E–H), at two temperatures and at constant electrolyte concentration (0.1 M $LiClO_4$). The small surface wave at +0.30 V versus Ag ($E°_{Os}$ is +0.72 V versus SSCE) in curves A, C, E, G represents charging of the polymer film to the poly$[Os(bpy)_2(vpy)_2]^{3+}$ state. The steady-state anodic waves for $[Fe(Me_2phen)_3]^{2+}$ oxidation are generally similar except (considering the differences in $[Fe(Me_2phen)_3]^{2+}$ concentration) currents are largest at naked electrodes in monomer DME and smallest at coated electrodes in polyether Me_2PEG-400. The limiting $[Fe(Me_2phen)_3]^{2+}$ oxidation currents at naked (I_{MT}) and coated (I_{LIM}) electrodes are used to calculate $k_{12}\Gamma$ (cm/s) from eq 2.

(25) Smyth, C. P. In *Dielectric Behavior and Structure*; McGraw-Hill: New York, 1955.

(26) (a) Marcus, R. A. *Annu. Rev. Phys. Chem.* **1964**, *15*, 155. (b) Marcus, R. A. *J. Chem. Phys.* **1965**, *43*, 679. (c) Marcus, R. A. *J. Phys. Chem.* **1963**, *67*, 853. (d) Marcus, R. A.; Sutin, N. *Biochim. Biophys. Acta* **1985**, *811*, 265. (e) In eq 6, $\log[f] = [\log K_{12}]^2/[4 \log(k_{11}k_{22}/Z^2)]$; taking $Z = 10^{11}$ M^{-1} s^{-1} and monomer k_{ex} values gives f ca. 0.5.

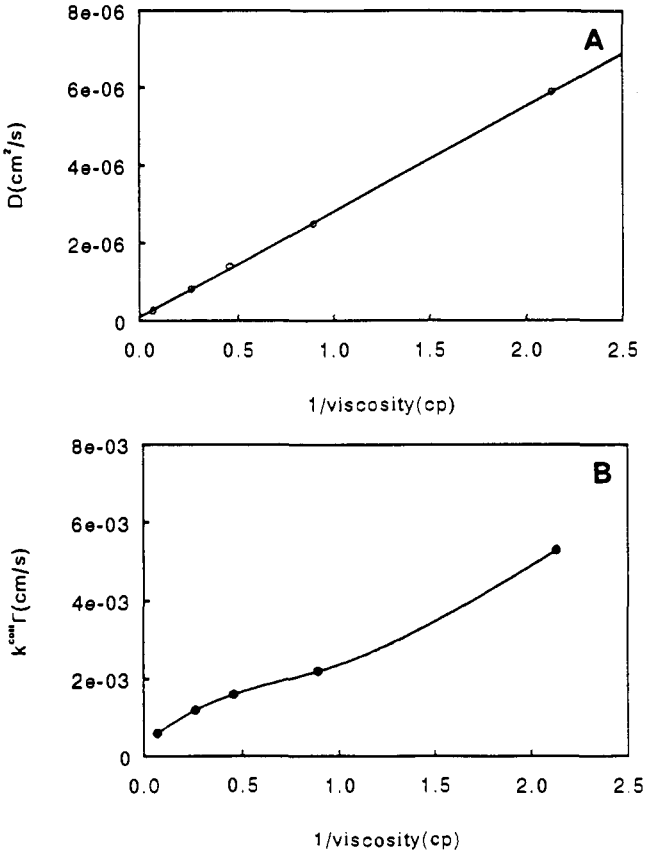

Figure 4. (Panel A) $[Fe(Me_2phen)_3]^{2+}$ diffusion coefficient, D_s, and (panel B) $k^{corr}\Gamma$ of reaction 1 versus reciprocal solvent viscosity.

Analogous voltammetry is seen in diglyme, triglyme, and tetraglyme solutions, except that $k_{12}\Gamma$ varies with solvent as shown (at 23 °C) in Table I along with the formal potential differences $\Delta E°$ and the normalized heterogeneous rate constants ($k^{corr}\Gamma$, vide supra). Table I additionally gives relevant solvent dielectric and viscosity properties and diffusion coefficients (D_s) of the iron complex calculated from naked microdisk currents (I_{MT}).

Values of $k^{corr}\Gamma$ measured for reaction 1, and of D_s of $[Fe(Me_2phen)_3]^{2+}$ (at 23 °C), are plotted in Figure 3 against the chain length of the ether solvent. Both dynamics parameters decrease with increasing solvent chain length, sharply at first and more gradually as the chain lengthens.

Polyether solvents of even higher molecular weight, Me_2PEG-1000 and Me_2PEG-2000, are waxy, partially crystalline solids at room temperature but melt to amorphous, viscous liquids at T_M = 35 and 52 °C, respectively. Microelectrode voltammetry was thus carried out in 55 °C melts. Raw and normalized rate constants, $k_{12}\Gamma$ and $k^{corr}\Gamma$, respectively, and D_s values for $[Fe(Me_2phen)_3]^{2+}$ at 55 °C in these polyethers and in DME, tetraglyme, and Me_2PEG-400 are reported at the right side of Table I. $k^{corr}\Gamma$ and D_s show dependencies on solvent chain length analogous to that in Figure 3. It is noticeable that while the diminution of $k^{corr}\Gamma$ becomes smaller for each successive doubling of chain length, the overall change in $k^{corr}\Gamma$ between monomer DME and Me_2PEG-2000 is quite substantial (50-fold at 55 °C). The parallel behaviors of $k^{corr}\Gamma$ and the $[Fe(Me_2phen)_3]^{2+}$ diffusion coefficient will be discussed later.

Viscosity. In monomer solvents, $[Fe(Me_2phen)_3]^{2+}$ diffusion coefficients vary inversely with solvent viscosity η as predicted by the Stokes–Einstein equation

$$D = kT/(6\pi R_h\eta) \quad (7)$$

where R_h is the hydrodynamic radius of diffusing $[Fe(Me_2phen)_3]^{2+}$ (8.2 Å). This relation is strictly applicable only when the diffusing species is large compared to the solvent molecules. Figure 4A shows 23 °C D_s data from Table I plotted according to eq 7; $[Fe(Me_2phen)_3]^{2+}$ diffusion in the small polyether solvents again obeys the Stokes–Einstein relation. R_h = 8.0 Å obtained from the slope of Figure 4A is similar to the earlier[1] monomer solvent result.

Table II. Electron-Transfer Rate Constants for Reaction 1 and Diffusivity of $[Fe(Me_2phen)_3]^{2+}$ as a Function of Electrolyte Concentration

electrolyte $[LiClO_4]$ concn	2 mM	0.01 M	0.1 M	1 M
D_s[a] (cm²/s)	2.5×10^{-7}	2.4×10^{-7}	1.9×10^{-7}	8.5×10^{-8}
$k^{corr}\Gamma$[b] (cm/s)	1.0×10^{-3}	7.6×10^{-4}	4.8×10^{-4}	1.6×10^{-4}
electrolyte $[Zn(CF_3SO_3)_2]$ concn	1 mM	0.01 M	0.1 M	0.4 M
D_s[a] (cm²/s)	2.4×10^{-7}	2.0×10^{-7}	1.6×10^{-7}	9.4×10^{-8}
$k^{corr}\Gamma$[b] (cm/s)	1.4×10^{-3}	1.1×10^{-3}	7.3×10^{-4}	3.6×10^{-4}

[a] Diffusion coefficient of $[Fe(Me_2phen)_3]^{2+}$. [b] Heterogeneous electron-transfer rate constant of reaction 1 normalized to $\Delta E°$ = 0.170 V.

Figure 4B compares the electron-transfer cross-reaction rate constant $k^{corr}\Gamma$ to reciprocal viscosity, revealing a rough correlation. Such a dependence might crudely be anticipated from the relation[25] between solvent longitudinal and Debye relaxation times

$$\tau_L = \tau_D(\epsilon_\infty/\epsilon_s) = (\epsilon_\infty/\epsilon_s)4\pi a_s^3\eta/kT \quad (8)$$

The dielectric properties of the polyether solvents in Figure 4B do not vary widely, in contrast to the previously studied[1] monomer solvents where dielectric constants varied widely and where there was no correlation between the reaction rate constant of reaction 1 and solvent viscosity. The Figure 4B result is analogous to several recent reports[6b,c,7c,8] including one in which sucrose was used to manipulate aqueous viscosities.

Variation of $k^{corr}\Gamma$ with Electrolyte Concentration. In a polymer electrolyte, including polyethers containing dissolved metal salts, the ionic conductivity of the electrolyte is moderated by the transient coordinative metal ion cross-linking ether dipoles on the same or on adjacent polymer chains.[9] The dipole coordination suppresses chain flexibility, especially at high electrolyte concentration, resulting in elevated T_G and increased tendency toward crystallinity, and, for the present purposes, increased chain segment relaxation times[14-18] and lowered diffusion coefficients of redox solutes.[10] A hypothesis in the present study is that such coordinative cross-linking might also be manifested in a change in effective polyether dipole fluctuation rates and accordingly in $k^{corr}\Gamma$.

$k^{corr}\Gamma$ and D_s were measured in Me_2PEG-400 containing from 2 mM to 1 M concentrations of lithium perchlorate and from 1 mM to 0.4 M concentrations of zinc triflate. The results, summarized in Table II, show that in both Me_2PEG-400/$LiClO_4$ and Me_2PEG-400/$Zn(CF_3SO_3)_2$ solutions, $k^{corr}\Gamma$ and D_s values decrease with increasing electrolyte concentration. The changes in $k^{corr}\Gamma$ again parallel those in D_s, and it seems evident that electron-transfer rate and physical diffusivity respond similarly to the buildup of a three-dimensional network by cation–ether coordination that lowers the local flexibility of polymer chains. These results are consistent with Brillouin scattering[14-16] studies that show a substantial increase in poly(propylene oxide) structural relaxation times as $LiClO_4$ electrolyte concentration is increased.

Electrolyte concentration changes may, on the other hand, have several additional effects on the electron-transfer rate measurement. At the lowest concentration, the electrolyte and electroactive species $[Fe(Me_2phen)_3]^{2+}$ concentrations have similar values, and electrostatic migration may contribute to the mass transport flux (I_{MT}). Examination of the relevant equation[27]

$$i_{MT,app} = i_{MT,true}/(1 + t_{Fe}) \quad (9)$$

shows that, if the transference number t_{Fe} is not negligible, I_{MT} will be overestimated and accordingly $k^{corr}\Gamma$ underestimated. If t_{Fe}, t_{Li}, and t_{ClO_4} are not very different, we estimate that a migration correction at 0.001 M electrolyte would be ca. 30%, in the direction

(27) Bard, A. J.; Faulkner, C. R. *Electrochemical Methods*; John Wiley: New York, 1980.

Table III. Temperature Dependence of Cross-Reaction Electron-Transfer Rate Constants and Diffusivity in 0.1 M $LiClO_4/Me_2PEG$-400

temp, °C	D_s,[a] cm^2/s	η,[b] cP	$\Delta E°$,[c] V	$k_{12}\Gamma$,[d] cm/s	$k^{corr}\Gamma$,[e] cm/s
60	4.5×10^{-7}	7.8	0.197	1.7×10^{-3}	2.8×10^{-3}
49.5	3.7×10^{-7}	10.1	0.222	6.9×10^{-4}	1.9×10^{-3}
40	3.1×10^{-7}	13.6	0.202	7.0×10^{-4}	1.3×10^{-3}
30	2.2×10^{-7}	19.1	0.198	5.1×10^{-4}	9.0×10^{-4}
23	1.9×10^{-7}	23.2 (24°)	0.219	1.9×10^{-4}	4.8×10^{-4}

[a] Diffusion coefficient of $[Fe(Me_2phen)_3]^{2+}$. [b] Arrhenius plot gives $\Delta G^{\ddagger} = 6.1$ kcal/mol; analogous plot for Me_2PEG-400 with no dissolved electrolyte gives $\Delta G^{\ddagger} = 5.2$ kcal/mol. [c] Formal potential difference, $\Delta E° = E°_{Fe(III/II)} - E°_{Os(III/II)}$. [d] Heterogeneous rate constant, uncorrected for variation in $\Delta E°$. [e] Heterogeneous rate constant of reaction 1 normalized to $\Delta E° = 0.170$ V.

of modestly increasing the observed electrolyte concentration dependency of $k^{corr}\Gamma$.

Increased electrolyte concentrations are known to enhance electrostatic screening and thus increase the electron-transfer rate between like-charged reactants,[28] and to enhance ion pairing of reactants which may act in the opposite direction to decrease reaction rates.[29] The former effect is opposite to and, while it may affect its magnitude, cannot account for the trend in Table II. Ion pairing of low concentrations of electrolytes in polyether solutions is minimal[16,17] but may occur, as may that of the metal complex reactants, at the higher concentrations employed. We observe, however, almost no change in MLCT electronic transitions for $[Fe(phen)_3]^{2+}$ in Me_2PEG-400, either pure (514 nm), 0.1 M $LiClO_4$ (515 nm), or 0.1 M $Zn(CF_3SO_3)_2$ (512 nm). Nonetheless, it must be admitted that interpretation of the electrolyte concentration dependency of $k^{corr}\Gamma$ as simply a polymer chain dynamics effect is complicated by these other phenomena, the most problematic of which is ion pairing.

Temperature Dependence of D_s and of $k^{corr}\Gamma$. The 23 °C to 60 °C temperature dependencies of $k^{corr}\Gamma$ for reaction 1, again corrected to $\Delta E° = 0.170$ V, of D_s of $[Fe(Me_2phen)_3]^{2+}$ in 0.1 M $LiClO_4/Me_2PEG$-400, and of the polymer solvent viscosity are reported in Table III and for the former two in Figure 5 as Arrhenius plots. The Arrhenius plots give activation energies ($\Delta G^{\ddagger}$) for electron transfer, diffusion, and (not shown) viscosity in Me_2PEG-400/$LiClO_4$ solutions of 8.9, 5.0, and 6.1 kcal/mol, respectively.

Two useful comparisons can be made from these results. Firstly, the D_s and η results of Table III form a linear relation according to eq 7, as did those of Table I (e.g., Figure 4A). That the activation energies for diffusion of $[Fe(Me_2phen)_3]^{2+}$ in, and viscosity of, 0.1 M $LiClO_4/Me_2PEG$-400 are similar, coupled with the eq 7 results, indicates that diffusion and viscous flow both reasonably reflect the polymer solvent chain dynamics and relaxation time τ_L.

Secondly, these activation energies can be compared to that for electron transfer (8.9 kcal/mol) after subtracting away the energy for the electron-transfer uphill reaction ($\Delta G_{RXN} = -nF\Delta E° = 5.07$ kcal/mol in Me_2PEG-400), leaving a residue of 3.4 kcal/mol. Presuming negligible inner-shell terms, this residue should measure the solvent reorganizational energy for electron transfer in (1) in Me_2PEG-400 polymer solvent. It is interesting that this barrier energy is *smaller* than those for diffusion and viscous flow which suggests that polyether "τ_L" values estimated by viscosity and diffusion would overestimate the "τ_L" that influences the electron-transfer rate (e.g., eqs 3–5). This result seems qualitatively reasonable: that the thermal requirements for polyether chain dipolar fluctuations attendant to crossing the electron-transfer barrier are smaller than those of the presumably larger nuclear displacements involved in chain segmental motions required to support viscous flow or physical diffusion of the electron-transfer reactant $[Fe(Me_2phen)_3]^{2+}$.

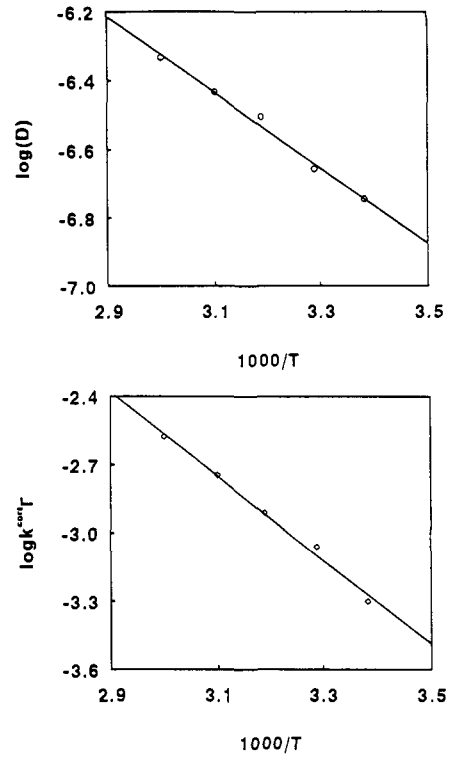

Figure 5. Arrhenius plots of D_s of $[Fe(Me_2phen)_3]^{2+}$ and of $k^{corr}\Gamma$ of reaction (1) in 0.1 M $LiClO_4/Me_2PEG$-400.

The electron-transfer plot (Figure 5B) also gives a preexponential factor $A = 941$ cm/s from which we calculate $K_p\kappa_{el}$ through eqs 3–5, taking τ_L as 22 ps, as 0.19 M^{-1} s^{-1}. This value is very close to the often used value[5a,30] 0.26 M^{-1} s^{-1} for homogeneous self-exchange electron-transfer reaction.

Discussion

Our previous work[1] showed that k_{12} for reaction 1 quantitatively responds to the characteristic dipolar relaxation rates, τ_L, of monomer solvents according to eqs 3–5 and that, based on this correlation, the effective dipolar relaxation time τ_L' for the polyether solvent Me_2PEG-400 was estimated as 22 ps. Analogous estimates of τ_L' for the other polyethers (Table I) indicate that the reaction scheme of Figure 1 serves to probe quite fast polymer chain motions.

The present experiments were conducted with the notion that increased polyether chain length and increased electrolyte concentration should systematically depress chain segment mobility and thereby lengthen the ether dipole fluctuation timescale. The results for $k^{corr}\Gamma$ in Tables I and II and Figure 2 are entirely consistent with this hypothesis and show that electron-transfer barrier-crossing rates can be predictively manipulated in polyether solvents via known dynamics aspects of the polymer phase.

A second important observation is found in the diffusion rate measurements (D_s). It is well-established[9,10] that solute diffusivity in polymer solvents is controlled by chain segmental mobility, and that D_s decreases with increase in polyether chain length and/or electrolyte concentration. The detailed chain segmental motions that control diffusivity of a solute through the polymer network and those that control ether dipole fluctuation rates are, as noted above, probably not the same, but that they are nonetheless related in their timescales is shown strikingly in Figure 6, where we plot all available $k^{corr}\Gamma$ data against the corresponding $[Fe(Me_2phen)_3]^{2+}$ diffusivity results. The data sets fall into clearly

(28) Brown, G. M.; Sutin, N. *J. Am. Chem. Soc.* **1979**, *101*, 883.
(29) (a) Lewis, N. A.; Obeng, Y. S. *J. Am. Chem. Soc.* **1988**, *110*, 2306. (b) Kozik, M.; Baker, L. C. W. *J. Am. Chem. Soc.* **1990**, *112*, 7604. (c) Blackbourn, R. L.; Hupp, J. T. *J. Phys. Chem.* **1990**, *94*, 1788.
(30) (a) Hupp, J. T.; Weaver, M. J. *J. Electroanal. Chem.* **1983**, *152*, 1. (b) Sutin, N. *Progr. Inorg. Chem.* **1983**, *30*, 441.

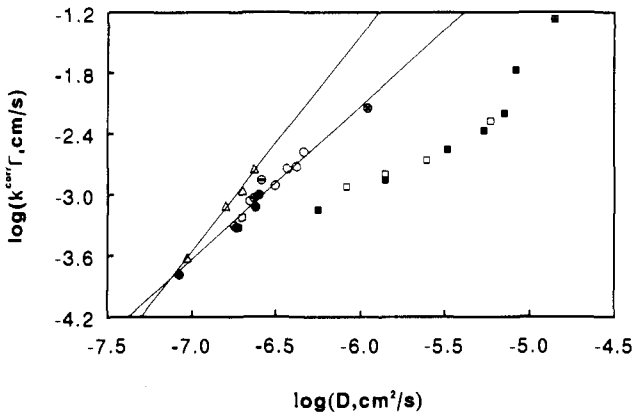

Figure 6. Log ($k^{corr}\Gamma$) versus log (D_s) for the data in $CH_3(OCH_2CH_2)_nOCH_3/LiClO_4$ solvent series (□) at 23 °C (Table I); in DME/$LiClO_4$ (□), tetraglyme/$LiClO_4$ (⊗), Me_2PEG-1000/$LiClO_4$ (⊖), and Me_2PEG-2000/$LiClO_4$ (⊕) at 55 °C (Table I); in Me_2PEG-400/$LiClO_4$ (●) and in Me_2PEG-400/$Zn(CF_3SO_3)_2$ (△) at different electrolyte concentrations (Table II); in Me_2PEG-400/$LiClO_4$ (○) at different temperatures (Table III) and in Me_2PEG-400/CH_3CN mixture solutions (■) (ref 1). The lines are drawn only to aid in recognizing different groups of data.

correlated groups; variations in $k^{corr}\Gamma$ and D_s with chain length at 23° (□) and at 55 °C (⊕, ⊖, ⊗, □) form two roughly parallel lines with unity slope, whereas variations in $k^{corr}\Gamma$ and D_s with electrolyte concentration ($LiClO_4$ (●) and $Zn(CF_3SO_3)_2$ (△)), in Me_2PEG-400/$LiClO_4$ with temperature (○), and in Me_2PEG-400/$LiClO_4$ with added CH_3CN (■, previous data[1]), form individual correlation lines with varied but >1 slopes. While there are clearly subtle controlling effects in relaxation timescales that produce these groupings, the main point is clear; electron-transfer rate, as controlled by dipolar fluctuation rate, and diffusion, as controlled by chain segmental mobility, are within a given set of experimental conditions tightly correlated.

The importance of reaction adiabaticity in controlling the effect of monomer solvent τ_L on reaction rates was pointed out recently by Weaver.[3d] A final comment on this matter is in order since we have recently described[11] electron self-exchange dynamics between tetracyanoquinodimethane and its radical anion that showed a correlation between reaction rate ($k_{ex}\delta^2$) and reactant diffusivity (D_s) reminiscent of the present Figure 6, but occurring over a much larger, (10^5-fold) range. The TCNQ results were interpreted as long-distance electron transfers provoked by a combination of large $TCNQ^{0/-}$ self-exchange rate constant and very slow reactant diffusion rates; this reaction is thus nonadiabatic. It is, on the other hand, relatively easy to show that the diffusion and electron transfer rates of reaction 1 are such that electron transfer is expected to occur at collision contact. Based on this and previous[19] observations, reaction 1 should be reasonably adiabatic in the polyether solvent and the analysis here is not to be confused with the TCNQ case.

Acknowledgment. This research was supported in part by grants from the National Science Foundation and the Department of Energy.

Importance of the Anisotropy of Atoms in Molecules for the Representation of Electron Density Distributions with Lewis Structures. A Case Study of Aliphatic Diazonium Ions

Rainer Glaser* and Godwin Sik-Cheung Choy[1]

Contribution from the Department of Chemistry, University of Missouri, Columbia, Missouri 65211. *Received March 30, 1992*

Abstract: The bond formation between a cation X^+ and an electron donor D is examined as a function of the electron acceptor capability of X^+ with topological electron density analyses at the RHF and MP2 levels. Atom populations *and* atom dipoles are important for the description of dative bond formation. Dative bond formation is manifested primarily in the anisotropy of the donor basin for weak acceptors X while charge transfer becomes important for stronger acceptors. Other population analyses allow for the estimation of *bond polarity* but neglect the importance of *atom polarities*. The different stages of dative bond formation are exemplified by analysis of the electron density distributions of heterosubstituted diazonium ions $(X-N_2)^+$ with different acceptors X and by analysis of charge transfer and of atom anisotropies as a function of progressing X-N bond formation. Various Lewis structures are discussed as representations of the electron density distributions resulting from X-N bonding. The consideration of X-N nonconnected Lewis structures is required to adequately represent the electron density distributions. Atom anisotropies also play an important role for the correct appreciation of electron correlation effects on the basis of integrated atomic properties.

Introduction

Molecular charge distributions play an important role in discussions of bonding and reactivity. Lewis structures are commonly used in these discussions although the *formal* charges in the Lewis structures may not represent the charge distribution correctly. Carbon monoxide is a well-known example. It is thus of great significance to establish relations between the electron density distribution and the Lewis structures. The consideration of bond polarities based on electronegativity differences or the consideration of different valence bond structures are attempts in this direction, but often it is difficult to reconcile[2] the two descriptions, and their apparent inconsistency has received considerable recent attention.[3] The general task is a difficult one as such a generalization would have to provide for a prescription as to how the electron density

(1) (a) Presented in part at the 25th Midwest Regional Meeting of the American Chemical Society, Manhattan, KS, Nov 1990. (b) Part of the projected Ph.D. dissertation of G. S.-C. Choy.

(2) Glaser, R. *J. Comput. Chem.* **1990**, *11*, 663.

(3) Wiberg, K. B., et al. *J. Am. Chem. Soc.* **1992**, *114*, 831, 841 and references therein.

0002-7863/93/1515-2340$04.00/0